MODELLING OF REALISTIC THREE DIMENSIONAL DAM COLLAPSE AND LANDSLIDE EVENTS

Paul W. Cleary*, Kai Rothauge and Mahesh Prakash

CSIRO Mathematical and Information Sciences, Private Bag 33, Clayton South, VIC 3168, Australia

ABSTRACT:

Computational modelling of extreme particle and fluid flow events can provide increased understanding of their post-initiation course. For the prediction of fluid events such as dam breaks we use the Smoothed Particle Hydrodynamics method, which is very well suited to the resulting complex highly three dimensional free surfaces flows, involving splashing, fragmentation, and interaction with complex topography and engineering structures. The prediction of landsides, which are collisional flows of rocks, is performed using the Discrete Element Method. Two case studies of dam breaks and one landslide event demonstrate the level of prediction that is now possible using these simulation methods.

1. INTRODUCTION

Extreme flow events such as flooding inundation resulting from the failure of a dam structure and from landslides can have significant impact on the people and environment of the affected region. The economic and human costs can be substantial. Computational modelling of these events can provide increased understanding of the post-initiation course of these extreme flow events. It can be used as part of risk management to characterise the likely outcomes from specific levels and types of failure in a range of anticipated scenarios. The effectiveness of various mitigation strategies can also be evaluated. To meet these needs the simulations require a high degree of realism and accuracy. For the prediction of fluid events such as dam breaks we use the Smoothed Particle Hydrodynamics method, which is very well suited to the resulting complex free surfaces flows, involving splashing, fragmentation, three dimensional bore structures and overtopping of hills all driven by the interaction of the fluid motion with the complex topographical features found in real mountain and valley regions. The prediction of landsides, which are collisional flows of rocks, is performed using the Discrete Element Method.

The most common method for modelling fluid based extreme flows is using the shallow water equations (Begnudelli and Sanders, 2006 and Begnudelli et al, 2008). In this approach the vertical dimension is averaged away to leave a two dimensional system of flow equations. These can be solved using grid based methods. They perform well when the fluid is relatively thin and covers large areas, but are not able to capture complex three dimensionality of the flow in regions such as flow through dam breaches, inundation of coastal structures or interaction with buildings, bridges and other infrastructure. To resolve three dimensional behaviour one can use a grid based method with some form of free surface tracking, such as level set (Osher and Sethian, 1988) or volume of fluid method (Hirt and Nichols, 1981). These methods though tend to be diffusive and do not conserve mass for finer flow structures and fragments. SPH is a Lagrangian particle based method that is easily able to capture complex three dimensional flow structures, including surface fragmentation and merging without such diffusive effects. SPH is therefore better able to capture fine and meso-scale flow structure and is highly suited to inundation problems such as tsunami impact on coastlines (Cleary and Prakash, 2004).

SPH was first extended to model incompressible free surface flows by Monaghan (1994). A simple two dimensional dam break was one of the original test problems and has been used extensively by many authors since then. SPH was first used to model three dimensional dam collapses with realistic topography (from a digital terrain model) for a hypothetical dam located in northern California by Cleary and Prakash (2004). This showed that simulation of large scale flooding from dam break was feasible. For details of the method and its applications see Cleary et al (2007) and Monaghan (2005). Here we continue the work by predicting the flood behaviour of a real 1928 collapse of the St Francis dam in Southern California (Rogers, 2008) and to model a catastrophic collapse scenario for a real dam at Geheyan in China.

Landslides are an important class of natural disaster that can lead to significant loss of life and significant property damage. Understanding the run-out path and the damage foot print of a specific landslide scenario enables estimates of economic, infrastructure and human loss to be made. In conjunction with suitable scenario planning a picture of the overall range of outcomes can be made. Various options for mitigation strategies can be explored and the effectiveness of specific protective structures (such as channels and walls) can be evaluated. The path that any specific landslide may take and how far it will run are key predictions that are needed to facilitate these outcomes.

A class of landslides that is particularly dangerous due to the very long distances they can travel and their very large rock volumes are known as long run-out landslides. Cleary and Campbell (1993) first used the Discrete Element Method (DEM) and showed that this scenario was possible through use of a very simple two dimensional DEM model with periodic boundaries. Campbell et al. (1995) used large scale two dimensional DEM simulations of the mountain slope and valley flow to further explore the phenomena.

---

* Corresponding author. Paul.Cleary@csiro.au

This modelling was extended to three dimensions using real topography by Cleary (2004) and Cleary and Prakash (2004). For more details on this method see Cleary (1998, 2004).

2. THE ST. FRANCIS DAM COLLAPSE

2.1 Background

The St Francis Dam disaster was arguably the worst American civil engineering failure of the 20th century. The catastrophic failure of this dam occurred on 12 March 1928 at 23:57:30h. It led to the loss of at least 450 people in the resulting floods. Located in the San Francisquito Canyon, about 15km north of Santa Clarita, California, the St Francis Dam was a curved concrete dam that was constructed between 1924 and 1926. The dam wall was 57m high, 213m long and had a stepped face, and at the time of failure the reservoir contained an estimated 47 million m³ of water, with a reported elevation of 559.4m (Outland, 1977). Figure 1 shows the dam before its failure.

Figure 1: The St Francis Dam before failure, looking north (Courtesy of Santa Clarita Valley Historical Society/ SVCHISTORY.com).

There were several factors that led to the dam collapse, the most important of which is that the dam wall was built on a poor foundation. Although modern geologists know that the type of rock found in the San Francisquito Canyon is unsuitable for a dam and a reservoir, two of the world's leading geologists of the time found no problems with it. The west abutment was built directly over San Francisquito earthquake fault, while the east abutment was built on a paleolandslide made up of mica schist that was interspersed with talc, giving it a greasy structure (Outland, 1977).

Figure 2: The St Francis Dam after failure, looking east. Note the central "Tombstone" remnant of the dam wall and the landslide scarp on the right-hand side of the image (Courtesy of Santa Clarita Valley Historical Society/SVCHISTORY.com).

It is now generally believed that the east abutment collapsed first (Outland, 1977 and Rogers 2008) the schist slowly creeping downward under the east abutment. Wetted conglomerates expanding under the west abutment pinched the dam wall like a vice, cracking it transversally in several places and lifting it up. Failure occurred when the schist formation began to slide and undercut the eastern side of the dam. As reported by Rogers (2008), in the most likely dam failure sequence, the eastern section of the dam wall crumbled as a flood wave started undercutting it and flowing along the downstream channel, carrying sections of the collapsed dam wall section with it. The remaining part of the dam wall tilted and rotated to that side, triggering a chain-reaction failure of the west abutment once the dam level had dropped by about 24m, releasing a secondary flood wave that quickly joined the primary one. What remained of the dam wall structure was the massive central section, nicknamed "The Tombstone". Figure 2 shows the dam after failure. As the flood wave surged down San Francisquito Canyon, it destroyed a hydroelectric power station located about 2km downstream of the dam site, as well as everything else in its path. It then followed Santa Clara Valley towards Ventura, where it finally reached the Pacific Ocean after travelling 87km in about five and a half hours.

2.2 Simulation domain

Digital terrain data was obtained from the USGS (2008) in the form of spatially uniform grid digital terrain models (DTM). For the San Francisquito Canyon, a 10m grid-resolution is available and is suitable for resolving all important topographic features. It was used in the simulation shown here. This area remains undeveloped and for the most part unchanged since the dam failure, so using modern terrain data should well represent the historical terrain, except for the dam wall region. This reflects changes due to the landslide on the eastern abutment at the time of failure and the subsequent undercutting of the dam wall that lead to the erosion of not only the landslide debris, but a 15m deep scour hole that was excavated once the landslide debris had been removed (Rogers, 2008). It is possible to modify the terrain mesh in this area to better reflect the initial conditions, but this idea was not considered important since the landslide debris, while initially plugging much of the breach, was quickly eroded by the outpouring water over a period of several minutes (Rogers, 2008). As the slide material eroded, the breach cross section was enlarged and the flow increased in magnitude. The wider initial breach will lead to a higher initial outflow with the peak outflow being reached more quickly. For canyon scale flooding prediction we do not expect this to have a large impact.

2.3 Flood Dynamics

The progress of the flood is shown in Figure 3. The water is coloured by its flow speed with dark blue being 0 m/s and red being 20 m/s. The channel in the upper reaches of the San Francisquito Canyon is tortuous and relatively steep (with a gradient of 2%). We restrict our discussion of the flood behaviour to this section of the canyon. The scenario modelled is of an instantaneous collapse of all the parts of the dam wall that failed. Within 10 s the leading water has collapsed and raced to around 200 m into the canyon. In the shallow valley just beyond the dam wall the flood front has a parabolic shape and is deeper and faster in the middle. At 1 min the flood front has travelled 0.5 km from the dam wall and has reached the opposite side of the valley. The water speed across most of the valley floor is around the 20 m/s maximum speed. The leading water which reached the far side has started flowing up the side

canyons walls, collapsing and then flowing back to the right. This leads to the first occurrence of a hydraulic jump where fast moving water coloured red interacts with a slow-moving region coloured green on the left and close to the leading edge.
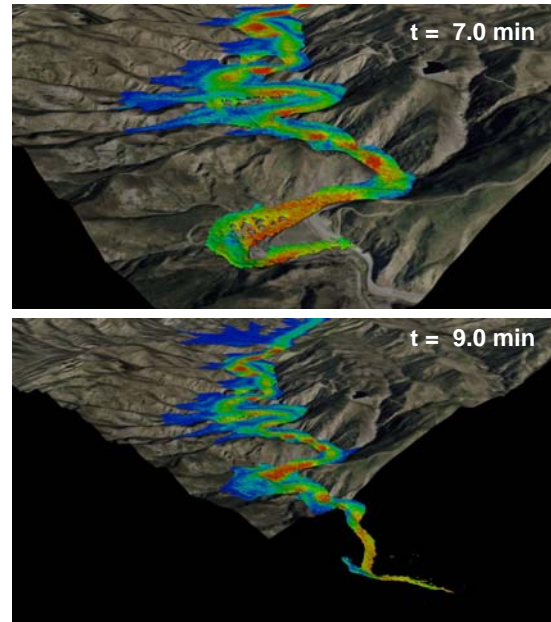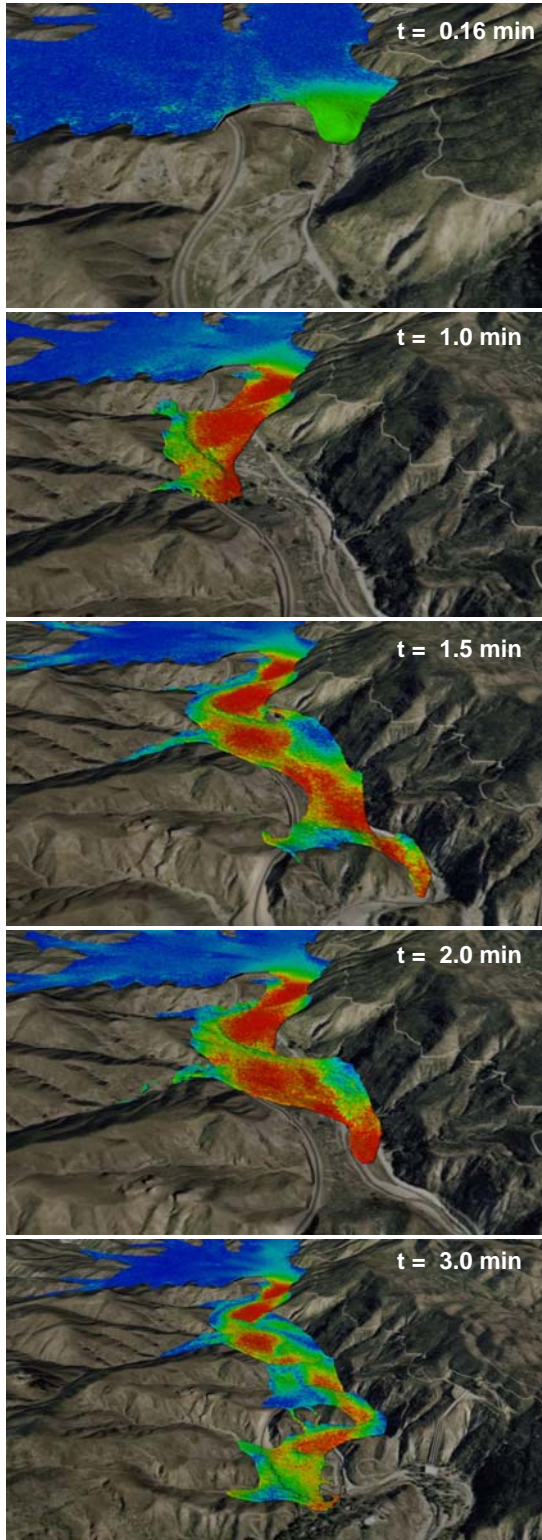

Figure 3: Flood wave travelling down the upper reaches of the San Francisquito Canyon. Blue is 0 m/s and red is 20 m/s.

At 1.5 min the flood front has progressed 0.8 km into the valley and has reflected back from the left canyon wall back across the valley flow and is now flowing along against the steep right wall of the canyon. The shape and location of the hydraulic jump has evolved significantly. With the increasing volume of water being reflected from the left, the jump has moved to the right and extended further down the valley. It makes contact with the right valley wall. On the front and left of the hydraulic jump the water level is significantly higher than in the valley floor region behind. So the water level does not at all decrease monotonically with distance from the dam breach. A substantial proportion of the water flows along the main valley but some water now starts to flood into two of the smaller tributary valleys to the left of the main valley.

At 2.0 min the water now stretches across a region of around 1.2 km of the main valley. There are now two hydraulic jumps with the original one close to the dam wall and a new one forming closer to the flood front. The position and structure of the first hydraulic jump have stabilised, but there is now a back flow from the location where it contacts the right wall of the canyon back upstream where it re-joins the flood in the valley floor. The momentum of the flood water presses the water up against the right wall of the canyon which records the highest water levels. The water then flows along this wall until it separates from the sharp bend in the foreground of this frame. The water then flows back across the now narrow canyon to the left wall where it is again reflected causing a second smaller hydraulic jump that passes diagonally across the valley. Water now begins to enter the large flatter side valley on the left in the foreground. The flooding of two of the earlier side valleys is now well advanced. Note that not all the side valleys on the left are flooding as this depends on the direction of flow and the water depth at the start of each valley. These are strongly influenced by the momentum of the water which in turn is controlled by its interaction with the valley walls encountered.

By 3.0 min the flood front has travelled about 1.5 km downstream of the dam. The leading water has now passed through a narrow 180° bend with a series of smaller hill peaks

on the left and then continues into a broad flatter section of valley. At this time, the broad open region of valley floor is almost flooded. The reflection of the water from its left side generates a third weaker hydraulic jump and water can be seen entering the two main side valleys. There are saddle type valleys between the last hills at the 180° bend mentioned earlier. These saddles form a natural barrier and the water piles up behind it, until a flood height of about 36 m above the channel floor is reached and the water starts spilling over. The overtopping of this saddle was observed from scour lines after the actual dam-break event and is predicted by the SPH model. The hill forming the southern canyon wall of this floodplain was finally completely overtopped at 7 min and remained overtopped for a substantial time. The flood front finally reaches the exit of the upper reaches of the San Francisquito Canyon after about 9 min, at which point it continues to flow through the topographically less interesting lower section of the canyon.

3. THE GEHEYAN DAM

3.1 Background

The Geheyan Dam is a concrete gravity arch dam built on the Qingjiang river, which is a tributary of the Yangtze river in Hubei Province in China. The dam wall is 206 m high and 653.5 m long and has a maximum capacity of 3.12 billion m^3 of water (Xu and Yan, 2004). This makes it one of the largest dams in the world in terms of reservoir capacity. In terms of capacity this dam is around 1000 times larger than the St. Francis Dam analysed in the previous section.

3.2 Simulation Domain

The DTM for the Geheyan Dam was obtained from USGS (2008) and has a resolution of 30 m. This was processed to remove pre-existing hydrological features with the help of CASM, China. For the preliminary simulation a partial section of the dam was used as shown in Figure 4. It consists of the central section of the Geheyan reservoir. The inundation region extends to the Changyang county on the left which is around 9 km from the dam and 6.3 km to the right of the dam. For this simulation a boundary resolution of 30 m and a fluid resolution of 15 m were used. The narrow and deep terrain in the Geheyan region makes it a very attractive model for dam flooding analysis using the SPH method since the resulting flow is expected to have significant three dimensional characteristics. For such dams therefore an SPH solution is expected to be significantly superior to a shallow water solution.
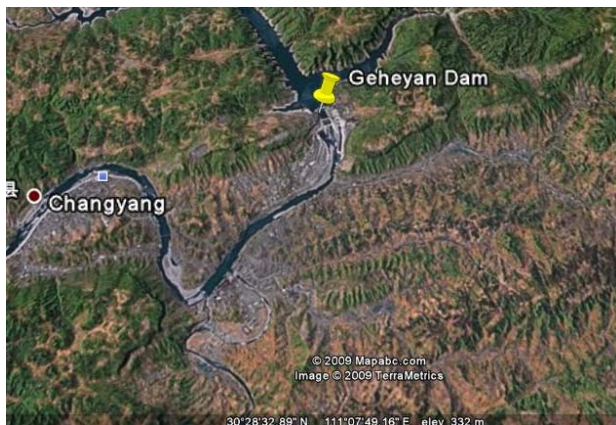

Figure 4: Location of the Geheyan Dam and the inundation region extending to the right to Changyang county.

3.3 Flood Dynamics

The progress of the flood wave after a possible complete dam collapse for the Geheyan Dam is shown in Figure 5. The water is coloured by its flow speed with dark blue being 0 m/s and red being 25 m/s. At 1.3 min the flood front has progressed by approximately 1 km into the main Geheyan valley. There are several side valleys along the main valley and the water has already filled one such small side valley on the right. At 3.8 min the main front has moved approximately 2.6 km towards Changyan county. Approximately 1.5 km downstream of the dam the flood waters splits into two parts, one feeding the main down hill branch on the left and another smaller up hill one on the right. The water also flood several smaller side valleys.

At 5.8 min the progression of the flood in the direction towards Changyan county on the left and a smaller stream to the right continues. The main branch now stretches approximately 5.4 km to the left filling most of the down stream valley down to the large bend at the bottom of the picture. In contrast, the uphill stream is only about 4.9 km long and is shallower and narrower. At around 4.8 km along the main valley a large wide side valley (at right angles to the main valley) is rapidly flooded. The potential of the SPH method to predict such complex branched flows is particularly advantageous in accurately determining inundation maps in such highly complicated terrains.

At 7.0 min the flood front in the main stream on the left has temporarily stopped progressing as the water fills a relatively flat but deep region. The right angle branch from the main valley further subdivides into two sections on either side of a mountain peak. The uphill branch has progressed further and is now 5.7 km long. The water level in the main valley continues to rise as the water escape rate from the dam still exceeds the flow rate along the various valleys at the flood front. More side valleys continue to be inundated.

At 10.0 min, the primary flow down the main valley again starts to progress towards the Changyan county after filling the large, flat depression. The right angle branch at the bottom has now slowed (water is now mostly blue here) and inundated broad areas to either side. The uphill branch on the right is now around 6.1 km long and has significantly broadened as some flatter valley flood plains have been inundated.

By 12 min a narrow fast moving stream of water develops in the main branch close to the flood front as water rushes through a very narrow section of the valley. The water in the lower right branch continues to slowly spread through the complex of valleys creating a large lake surrounding one mountain peak and almost surrounding a second. The flood levels in the main valley appear to have stabilised and the flow velocities are starting to decline. The flooding in the uphill valley branch continues steadily and is not discussed from here on.

At 14.2 min the leading edge of the flood has reached 7.7 km along the main Geheyan valley. It has broadened and slowed after moving past the constriction (where the flow is coloured red). The flooding in the lower right branch has now reached its peak with multiple peaks isolated in the flood.

At 20.0 min the flood front reaches Changyang county. The speed of the flood waters has significantly declined from its early level of around 25 m/s to a more moderate 10-12 m/s at the leading edge. Some retreat of the water in the lower right branch can be seen.

Finally, by 25.7 min the side valleys around the Changyan region have become substantially flooded as water from the main valley branches out into smaller tributaries. The total flooded region is now around 20 km long.

For the Geheyan Dam the complex three dimensional nature of the flood dynamics results in several branches of the flood. Constrictions and sudden depressions in the terrain result in alternative speeding and slowing of the flood front as water alternatively accelerates through narrow regions and floods broad low lying regions. The SPH method was easily able to predict the large scale flooding dynamics using realistic topography. In future work, we will extend the simulation domain to include the entire dam reservoir as well as a larger inundation region. Several collapse scenarios ranging from partial to progressive to complete collapse will be considered.
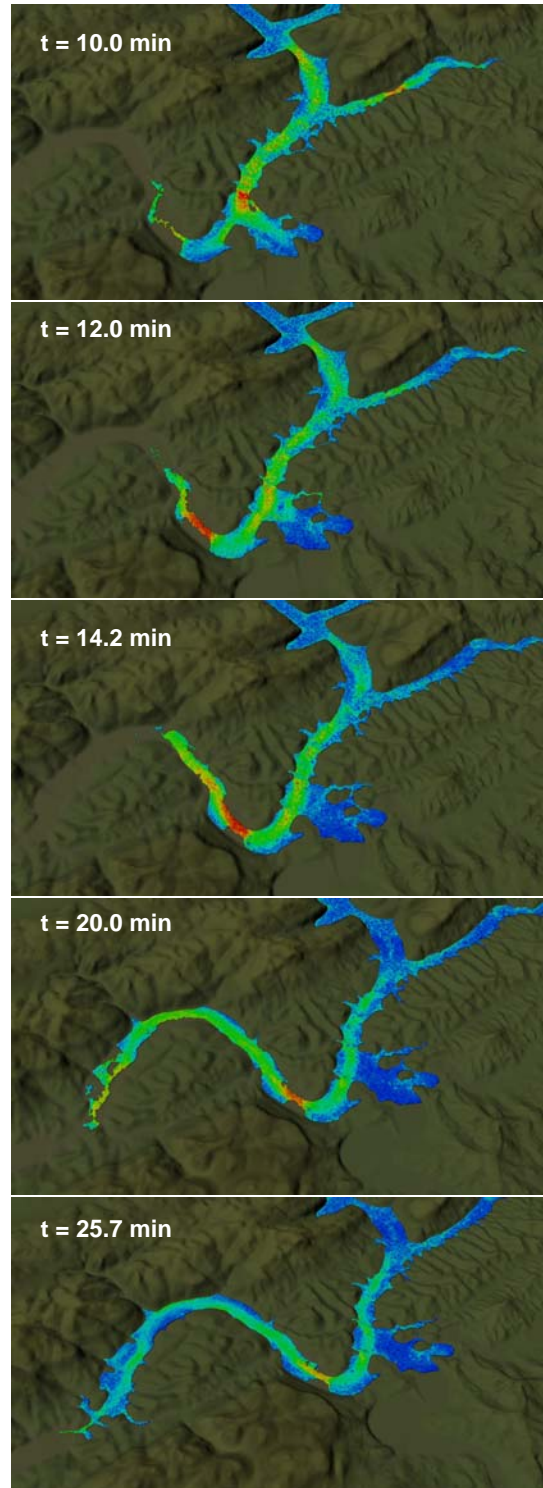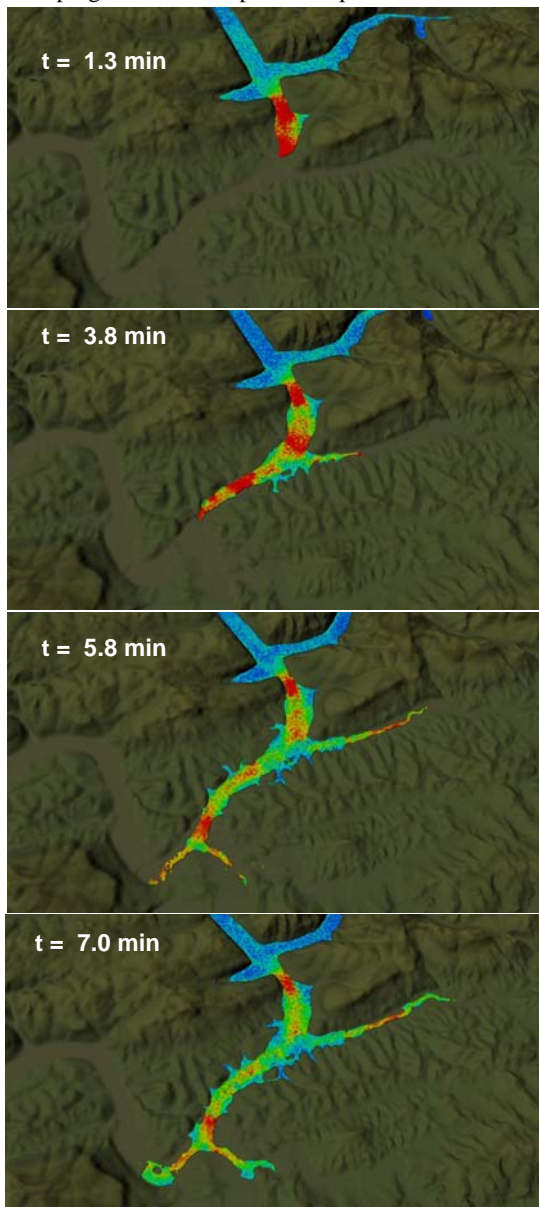

Figure 5: Progress of flood wave down the Geheyan valley. Blue is 0 m/s and red is 25 m/s.

4. LANDSLIDES

We re-visit a generic landslide event type – being the collapse of a mountain peak post fragmentation by an earthquake. This scenario was previously used to demonstrate DEM modelled in three dimensions on real topography (Cleary and Prakash, 2004), where the particles were represented as spherical grains. Here we predict the progress of the landslide when more realistic non-spherical particle shapes are used. For details of

the super-quadric particle representation see Cleary (2004). The blockiness used was 2.1-4.0, the intermediate axis aspect ratio was 0.9 and the small axis aspect ratio was 0.7-0.9. These particles vary from close to spherical to mildly elliptical to cubical to brick like. This is a moderate (not extreme) range of shape and is a plausible representation of naturally occurring rock fragments. The mass of rock in the landslide is 12 million tonnes. This represents a volume of 3.04 million m^3 and consists of 245,000 particles. The particle diameters are uniformly mass weighted between 2.0 m and 10.0 m with a mean diameter of 2.4 m. The friction coefficient used was 0.5 for both rock-rock and rock-ground collisions. A coefficient of restitution of 0.3 was used for rock-rock collisions while a slightly higher value of 0.5 was used for rock-ground. The spring stiffness used in the simulations was 10^9 N/m which gave average overlaps of 0.3% of the particle diameters.

Figure 6 shows the collapse of the mountain peak into a valley. The particles are coloured by their speed with blue being stationary and red being 50 m/s or higher. The initial peak was converted into a mound of particles that are then free to flow on the underlying topography. They collapse forwards and down two side valleys producing a left and right branch of the landslide, which are separated by a series of small peaks (labelled). By 20 s, the three branches all merge to create a single large flow of particles down the central valley. By 26 s, the supply of new material from the original peak location (now coloured dark blue) has slowed and the main landslide is moving at its peak speed (coloured red) and is approaching the valley flow where it comes to rest.
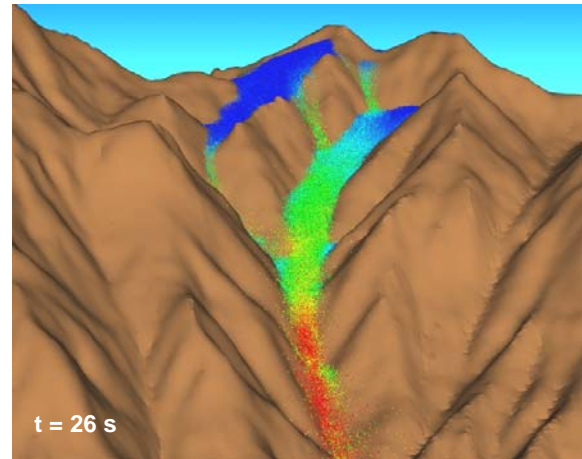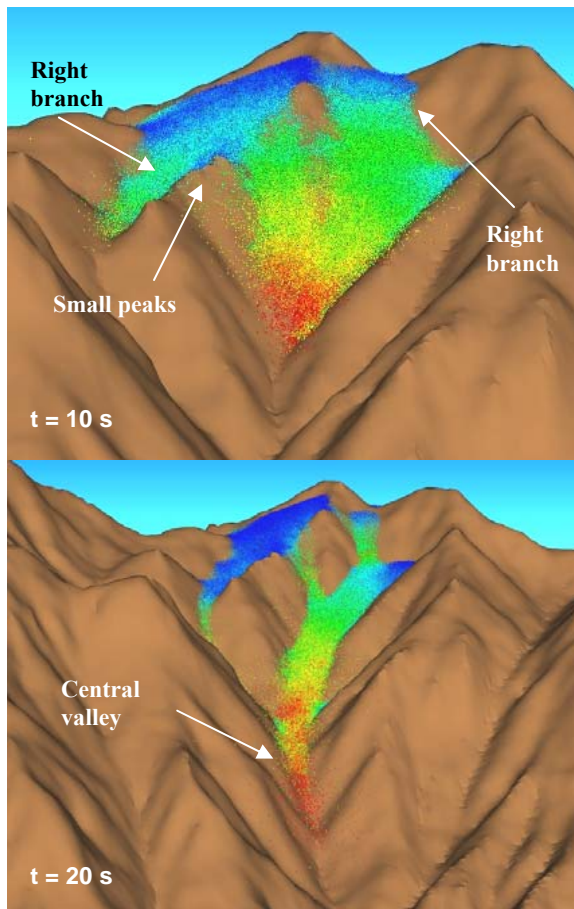

Figure 6: Landslide produced by a collapsing fragmented mountain peak using non-spherical particles at 10 s, 20 s and 26 s after landslide initiation.

5. CONCLUSIONS

SPH has been shown to be a very effective simulation tool for predicting post dam collapse flood inundation on a large scale and in circumstances where strongly three dimensional flow behaviour occurs. Simulation of the historical St Francis dam collapse demonstrates the ability to predict hydraulic jumps, overtopping of hills, back flow and inundation of side valleys. The predictions are consistent with the observed flood time scales including the timing of the destruction of a downstream power plant. Simulation of a hypothetical dam collapse of the massive Geyeham dam has also been presented. The flow is again complex with significant upstream flow and strong impact of the detailed topography on the progress of the flood and the flood heights reached in various locations. Finally, DEM prediction of the collapse of a mountain peak to form a large volume landslide has been demonstrated. In all cases, particles based methods are a powerful tool for exploring the consequences of specific catastrophic geophysical and civil engineering failures.

REFERENCES

Begnudelli, L., and Sanders B. F., (2006), "Unstructured Grid Finite Volume Algorithm for Shallow-Water Flow and Scalar Transport with Wetting and Drying", J. Hydraul. Eng., 132(4), 371-384.

Begnudelli L., Sanders B. F., and Bradford S. F., (2008), "Adaptive Godunov based Model for Flood Simulation", J. Hydraul. Eng., 134(6), 714-725.

Campbell, C. S., Cleary, P. W., and Hopkins, M. A., (1995), "Large scale landslide simulations: Global deformation,

velocities and basal friction", J. Geophys. Res., 100, B5, 8267-8283.

Cleary, P. W., and Campbell, C. S. (1993), "Self-lubrication for long run-out landslides: Examination by computer simulation", J. Geophys. Res., 98, No B12, 21911-21924.

Cleary, P. W., (1998), "Discrete Element Modelling of Industrial Granular Flow Applications", TASK. Quarterly - Scientific Bulletin, 2, 385-416.

Cleary, P. W., (2004), "Large scale industrial DEM modelling", Eng. Comp., 21, 169-204.

Cleary, P. W., and Prakash, M., (2004), "Smooth Particle Hydrodynamics and Discrete Element Modelling: potential in the environmental sciences", Phil. Trans. A, 362, 2003-2030.

Hirt, C. W., and Nichols, B. D., (1981), "Volume of fluid (VOF) method for the dynamics of free boundaries", J. Comput. Phys., 39, 201-225.

Monaghan, J. J., (1994), "Simulating free surface flows with SPH", J. Comput. Phys, 110, 399-406.

Monaghan, J. J., (2005), "Smoothed particle hydrodynamics", Rep. Prog. Phys., 68, 1703-1759.

Osher, S. and Sethian, J. A., (1988), "Fronts propagating with curvature-dependent speed: algorithms based on Hamilton-Jacobi formulation", J. Comput. Phys., 79, 12-49.

Outland, C. F., (1977), "Man-Made Disaster: The Story of The St Francis Dam", A.H. Clark Company.

Rogers, J. D., (2008), "Reassessment of the St Francis Dam Failure", http://web.mst.edu/~rogersda/st_francis_dam.

United States Geological Survey (USGS), (2008), "The National Map Seamless Server" http://seamless.usgs.gov/.

Xu, R., and Yan, F., (2004), "Karst geology and engineering treatment in the Geheyan Project on the Qingjiang River, China", Engg. Geology, 76, 155-164.